Appl. Phys. B 53, 221–225 (1991)

Applied Physics B Photophysics and Laser Chemistry

Laser-Induced Electron Emission from an Au Surface Irradiated by Single Picosecond Pulses at λ=2.94 μm. The Intermediate Region Between Multiphoton and Tunneling Effects

C. Tóth[1], **G. Farkas**[1], **and K. L. Vodopyanov**[2*]

[1] Central Research Institute for Physics, P.O. Box 49, H-1525 Budapest, Hungary
[2] General Physics Institute, Vavilov Str. 38, SU-117942 Moscow, USSR

Received 12 June 1991/Accepted 2 August 1991

Abstract. The photoinduced electron emission from the surface of a solid gold target irradiated by single picosecond pulses of an erbium laser is investigated. The applied laser intensity (5–120 GW/cm^2) corresponds to the intermediate interaction region between the pure multiphoton and tunnel effects, where the decisive Keldysh-parameter, γ, is in the range $1 < \gamma < 12 = n_0$. In the light intensity region which is free of surface heating ($I_L < 80$ GW/cm^2), the slope of the measured logarithmic intensity dependence of the photocurrent decreases from the $n_0 = 12$ perturbative value down to $n \cong 5$. Therefore the experiment shows that the Keldysh-type theories, which have recently been proved to describe correctly the ionization of atoms, are also valid to a certain extent in the case of the photoeffect in metals.

PACS: 32.80K, 79.20D, 79.60

The laser induced photoeffect in metals – as a simple model interaction – is a useful experimental tool [1–6] for investigations of the photon–electron interaction at high light intensities. Similarly to the case of multiphoton ionization of atoms (gases) by intense laser fields, the photoelectron emission from metals manifests itself in two different forms distinguished by the so-called Keldysh (or perturbation) parameter, γ [7, 8]; the latter is defined by $\gamma = \omega(2\,\mathrm{mW})^{1/2}/eE$, where W denotes the depth of the potential well ("work function"). m and e are respectively the mass and charge of the electrons, while ω and E are the frequency and the electric field strength of the laser light. One limiting case, $\gamma \gg 1$, for low light intensities and high frequencies represents the pure multiphoton mechanism, for which the interaction may be considered perturbatively. Here the order of nonlinearity is $n_0 = [W/\hbar\omega + 1]_{\mathrm{int}}$, which is equal to the minimum number of interacting photons required to produce one free electron. The other limit is the optical tunneling, where the electrons escape from the potential well by quantum mechanical tunneling through the barrier broken down periodically by the oscillating electromagnetic field. This case occurs for high laser intensities and low frequencies, when $\gamma \ll 1$.

Detailed experimental studies have been published for the pure multiphoton case using visible (ruby) and near infrared (Nd) nanosecond and picosecond lasers, respectively [2, 9]. The upper intensity limit of the perturbative region at $\lambda = 1$ μm [6], as well as for the tunneling case were determined, using far-infrared nanosecond lasers (CO_2, $\lambda = 10$ μm) [10].

As for the intermediate region between the two mentioned cases, we have previously reported on a first experiment at $\lambda = 2.8$ μm [11], when the Keldysh-parameter γ was on the order of 6. We used the pulse train of an actively mode-locked Er^{3+}:YSGG laser. In these experiments the heating of the metal surface by the laser radiation – caused by the accumulation of successive laser pulses of the train – significantly influenced the electron emission processes leading to thermally assisted photoelectron emission. For the $\gamma \cong 1$ transition region in the analogous case of ionization of atoms, results of two experimental works were published recently [12, 13]. These authors observed tunneling character even in the perturbative side ($\gamma > 1$) of the transition region. Similar quantitative measurements and comparison with theories are missing for the photoeffect at metal surfaces, with the exception of the level of [10, 11].

The aim of the present paper is to report on new experimental results for laser-induced electron emission of metal surfaces. We have continued our work in the intermediate intensity range between the perturbative and

* Present address: Experimental Physik III, Univ. Bayreuth, W-8580 Bayreuth, F.R. Germany

nonperturbative limiting regions of the interaction: an Au surface was investigated as a cathode using single, selected pulses of an actively mode-locked Er^{3+}:YAG laser at $\lambda = 2.94\,\mu m$ wavelength. In the first part of the present paper we also discuss our experimental results on the reflectivity of gold at $\lambda \cong 3\,\mu m$ and its temperature dependence for grazing angles of incidence. This point plays an important role in our photoemission experiments because of possible heating effects during the electron emission.

Our measurements of the intensity dependence of the photocurrent are described in the second section of the paper. We underline here the main differences between the previous [11] and the present investigations, which are the following: (i) here we use single pulses instead of a laser pulse train, to avoid accumulative heating; (ii) the application of a grazing angle of incidence, $\Theta \sim 89°$ (instead of $\Theta \sim 75°$), which leads to an approximately 15 times larger beam spot on the surface, and a further decrease of the possible heating effects; (iii) the laser intensities used are about 1–5 times higher here, in order to get closer to the $\gamma = 1$ value.

1. Measurement of Reflectivity of Gold at λ=3 μm

As the multiphoton electron emission in our case can be considerably affected by the temperature rise of the irradiated surface [11] the latter fact has to be calculated rather accurately. This implies that we should know at least the light absorption coefficient $A = 1 - R$ and its dependence on temperature. Knowing this value and the temporal shape of the laser pulse we may evaluate the temperature of the surface as a function of time by solving a heat diffusion equation.

The tabulated data for the optical absorption for Au at room temperature near 3 μm (normal incidence) scatter from $A_0 = 0.5$–3%, while data for the temperature dependence $A = A(T)$ are absent by now. For longer wavelengths (10.6 μm) the Drude-Zener theory of metals predicts, for temperatures higher than the Debye temperature, a linear increase of A with T, which is experimentally verified [14]. For shorter wavelengths this theory is not valid and the effect of the band structure and the anomalous skin effect should be taken into account, which can sometimes even lead to a decrease of A with T [15].

We have measured the room temperature reflectivity R and also the real and the imaginary parts of the index of refraction ($\varepsilon^{1/2} = n - i\kappa$) for thick, polished Au targets, using pulses of an erbium laser at 2.94 μm. A laser beam with s- or p-polarization was directed at grazing incidence (angle $\Theta = 70$–89°) onto the metal surface. The light intensity was chosen to be weak enough to avoid the heating of the metal. The reference and reflected signals were measured by linear thin film pyroelectric detectors.

Figure 1 shows the dependences of reflectivities of Au for s- and p-polarization versus angle of incidence Θ. The solid curves are theoretical ones with $n = 1.37$ and $\kappa = 20$, which provide the best fit to the experimental data. The procedure also takes into account the following relationships (see textbooks such as [16]): (i) for p-polarization $A(\Theta)$ reaches its maximum at the Brewster angle, $\Theta_B = \pi/2 - 1/\kappa$; (ii) the absorptivity at Θ_B is equal to: $A(\Theta_B) = 2n/\kappa$. From the experimental results we may also calculate the values of the Brewster angle, $\Theta_B = 87°$, and the absorption at normal incidence $A(\Theta = 0°) = 4n/\kappa^2 = 1.37\%$ (Au, $\lambda \cong 3\,\mu m$).

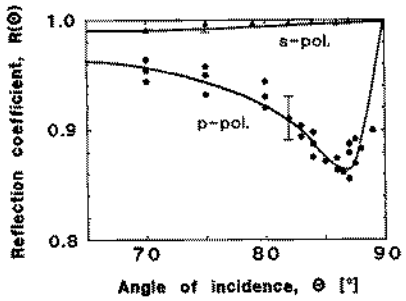

Fig. 1. Dependences of the reflectivity of gold for s- (▲) and p-polarization (•) at $\lambda \cong 3\,\mu m$ versus the angle of incidence, Θ. Solid curves: theoretical fit for $n = 1.37$ and $\kappa = 20$

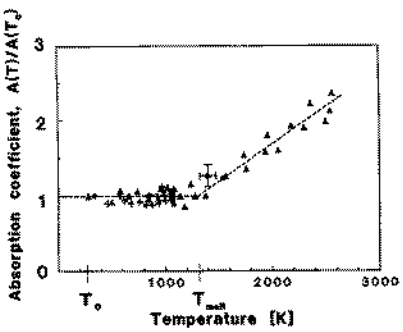

Fig. 2. Relative change of the absorbtivity, $A(T)/A(T_0)$, of gold at $\lambda \cong 3\,\mu m$ versus the surface temperature. +: laser train energy of 14 mJ; ▲: 18.5 mJ

We also measured the reflectivity of Au for grazing angles of incidence as a function of laser intensity in the range of 0–20 GW/cm^2. The gold surface was irradiated by a train of 100 ps pulses with the total duration (FWHM) of the envelope of 100–150 ns and for a fixed angle of incidence of $\Theta = 85°$.

The measured time evolution of the reflectivity throughout the train enables us to calculate the change of peak temperature of the surface from pulse to pulse using the general heat diffusion equation [17], and finally to compute the dependence of the reflectivity (or absorptivity) on temperature. We assume here that equilibrium exists between electron and lattice temperatures because of the small electron–lattice energy exchange time of 2–3 ps [18] as compared to the duration of the laser pulses.

Figure 2 presents the measured relative absorption change (averaged over time and spot size) $A(T)/A(T_0)$ versus the surface temperature T in the center of the laser spot and at the moment of the maximum laser intensity. Here T_0 is room temperature. Within the experimental accuracy, A does not depend on T up to the melting

point $T_{melt} = 1336\,K$; for larger values of T a linear dependence is found.

Theoretically there should be a step-like change of absorption at the melting point. In our case the distribution of laser intensity in time and space is Gaussian and the linear increase of the absorption after reaching the melting point in the center may be explained by the growth of the molten area with rising intensity.

In summary we can state that for picosecond pulses the reflectivity of Au in the 3 μm wavelength region does not depend on laser intensity unless the surface is heated up to the melting point. In the range of grazing incidence, $\Theta_B < \Theta < 90°$, we can essentially reduce the role of surface heating due to a decrease of absorption and an increase of the dimensions of the irradiated spot.

2. Laser-Induced Electron Emission from Gold

We now turn to a discussion of our photoeffect experiments. The experimental setup was similar to those of [3, 6, 11], now using single, cavity dumped pulses of an actively mode-locked Er^{3+}:YAG laser (cavity dumped version of the laser system described in [20]). The single pulse generated at $\lambda = 2.94\,\mu m$ wavelength has a duration (FWHM) of 110 ± 10 ps, close to the bandwidth limitation, and an energy of 0.5 mJ. The diameter of the beam is ~ 1 mm.

A beam-splitter divides the laser light into two parts: one for monitoring by a fast germanium photodiode, while the second part enters the target chamber (kept at $\approx 10^{-5}$ Pa) through a silica window. In the vacuum chamber a well prepared, polished gold cathode of 1 mm thickness is irradiated by the single laser pulse at grazing incidence, $\Theta \approx 89°$. The photoelectrons are collected by another gold plate with the same dimensions placed 1 cm away from the cathode and kept at a high extraction voltage (6–10 kV) in order to overcome the space charge limitations of the current [21]. The beam is focused onto the surface of the gold plate by a CaF_2 lens with focal length of 53 mm. The laser intensity I_L is varied between 5 and 120 GW/cm^2 at the sample surface by suitable filters. We apply p-polarized incident light – i.e., the electric field vector E of the light is almost perpendicular ($\Theta \cong 89°$) to the gold surface – to ensure the conditions for surface-type photoeffect. With these data the Keldysh-parameter, γ, defined in [7, 8] to distinguish between the pure multiphoton ($\gamma \gg 1$) and the pure tunneling approach ($\gamma \ll 1$) varies from 12 to 2.5, where $\gamma = \omega(2\,mW)^{1/2}/eE$; here we take into account the approximate doubling of the electric field amplitude of the light near the surface due to the almost perfect reflection from the metal surface.

The monitor signal is detected by a linear photodetector and a digital oscilloscope, while the induced photocurrent, j, is measured directly by a 50 Ω input resistance of a Tektronix-7104 oscilloscope.

Two typical dependences of the photoelectric current on the applied laser intensity are shown in Fig. 3.

Figure 3a corresponds to an intensity around $I_1 = 5\,GW/cm^2$, $\gamma = 12$, where a pure perturbative multiphoton photoeffect is observed with $n = 11.5 \pm 1 \cong n_0 = 12$

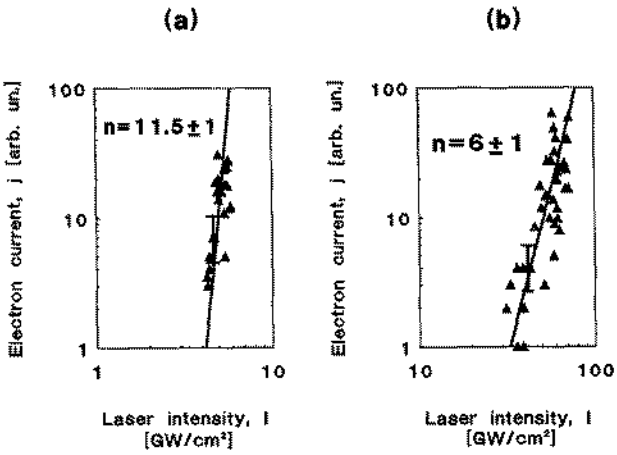

Fig. 3a, b. The photoemitted current as a function of the laser intensity around **a** $I_1 = 5\,GW/cm^2$, and **b** $I_2 = 63\,GW/cm^2$, with the fitted logarithmic slope values

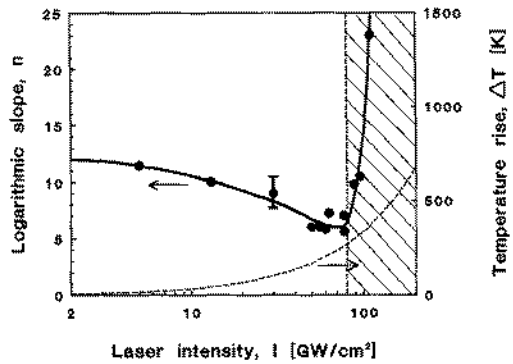

Fig. 4. The logarithmic slope values of the light intensity dependences of the photocurrent at various intensity regions. The circles are experimental points, the continuous line is a smooth fit to show the main tendencies. The shaded area represents the intensity region of the thermally assisted processes, which is also proved by the dashed curve in the bottom-right part of the figure: it shows the increase of the surface temperature in the laser spot region

($W_{gold} \cong 4.7\,eV$ and $\hbar\omega_{Er:YAG} = 0.418\,eV$, $n_0 = [W/\hbar\omega + 1]_{int} = 12$). Figure 3b on the other hand shows the situation around $I_2 = 63\,GW/cm^2$, $\gamma = 3.3$; here the observed slope, $n = 6 \pm 1$, is clearly different from the perturbative one, $n \neq n_0 = 12$. We have also determined the slope values $n = \partial \log j / \partial \log I$ at other laser intensities; the results are plotted in Fig. 4 (full experimental points, left-hand ordinate scale; details of the figure will be discussed below. It can be clearly seen, that up to $\sim 10\,GW/cm^2$ the slope n is practically constant, while above this intensity it starts to decrease. After reaching a minimum ($n \cong 5$) at $\sim 70\,GW/cm^2$, the slope starts to increase again, reaching $n = 23$ at $110\,GW/cm^2$. As we shall see below, the measured changes of the slope values can be interpreted by optical tunneling (decrease of n below $I \cong 10\,GW/cm^2$) and at higher laser intensity by the heating of the metal surface (increase of n above $80\,GW/cm^2$). As for the experimental comparison of the various polarization cases

of the incident light beam, using s-polarized light no photocurrent was observed ($< 10^5$ electrons) up to a laser intensity of $I_L = 150\,\mathrm{GW/cm^2}$.

3. Discussion

Taking into account that in our previous investigations the main disturbing processes were the thermal effects, let us look first at heating effects. Using the same calculation method as in [11] and the results discussed above for the absorption coefficient $A(\Theta)$, we may estimate the temperature rise of the surface in the middle of the laser spot at the moment of the maximum laser intensity. The maximum change of the surface temperature is evaluated to be proportional to the applied laser intensity, $\Delta T = 3.4 \times 10^{-9} \cdot I$ (I in $\mathrm{W/cm^2}$, ΔT in K). We note here that a possible temperature difference between the electrons and the lattice is neglected in our calculation; following the theory of [19] and with our data and those of [18], the difference is definitely less than 100 K and may be omitted. The estimated temperature rise of the surface is plotted in Fig. 4 as a function of the laser intensity (broken curve, right-hand ordinate scale).

Examining Fig. 4, a coincidence can be found between the region with positive slope of the $n(I)$ curve and the range where $\Delta T > 300\,\mathrm{K}$ (shaded area in the figure). This clearly shows the effect of the surface heating on the emission: below $\Delta T \sim 300\,\mathrm{K}$, the modification of the original Fermi distribution of the metallic electrons is of minor importance, while above $\Delta T \sim 300\,\mathrm{K}$ the emission process is notably modified by the changed electron energy distribution of the metal, leading to thermally assisted emission processes [5]. It is suggested that the shaded region of Fig. 4 represents thermally assisted processes. As a consequence, the comparison of our experimental results with the pure multiphoton or tunneling theories is restricted to the left part of Fig. 4, where $I < 80\,\mathrm{GW/cm^2}$. For the further discussions this "athermal" region of Fig. 4 is plotted again in Fig. 5.

Since the applied laser intensity range corresponds to an intermediate region ($1 < \gamma < 12$) between the pure photoeffect ($\gamma \gg 1$) and pure tunneling ($\gamma \ll 1$) situation, we have to use the complete theoretical formula for the comparison with our data. Based on Refs. [7, 8], we may write for the electric current (omitting preexponential factors):

$$j \propto \exp\left\{-\frac{2W}{\hbar\omega}\left[\left(1+\frac{1}{2\gamma^2}\right)\operatorname{arcsinh}\gamma - \frac{\sqrt{1+\gamma^2}}{2\gamma}\right]\right\}. \quad (1)$$

The logarithmic derivative then reads

$$n = \frac{\partial(\log j)}{\partial(\log I)} = \frac{W}{\hbar\omega}\cdot\left[\frac{1}{\gamma}\cdot\sqrt{1+\gamma^2} - \frac{1}{\gamma^2}\operatorname{arcsinh}\gamma\right]. \quad (2)$$

This dependence is shown in Fig. 5 as solid line (a). Obviously this curve does not fit the experimental points. However, introducing an effective value γ' (see [22]) in place of γ, the experimental points can be fitted completely with $\gamma' = \gamma/3$ [see curves (b) and (c) of Fig. 5 with $\gamma' = \gamma/3$ and $\gamma' = \gamma/9$, respectively].

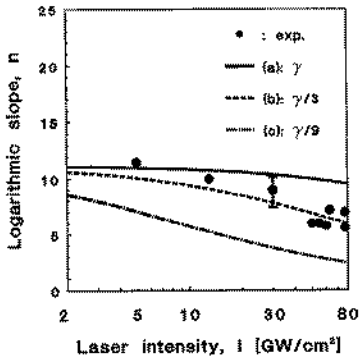

Fig. 5. The same as Fig. 4, but without the thermally influenced laser intensity region above $80\,\mathrm{GW/cm^2}$. The circles are experimental points, the fitted theoretical curves correspond to various γ values: *a* $\gamma = \gamma$; *b* $\gamma' = \gamma/3$; *c* $\gamma'' = \gamma/9$

The reasons for the concept of a new, "dynamic" value of the work function $W' < W$ in a metal and correspondingly a new $\gamma' < \gamma$ parameter are also discussed in [10, 22–24]. One possible mechanism of the laser-induced change of the work function is a certain internal excitation of the metallic electrons, e.g. by inverse Bremsstrahlung effects [22]. Another cause for the disagreement between the theoretical and experimental data in Fig. 5 is the approximate nature of the formulae used in the transition region. General theories describing the nonlinear photoeffect [7, 8] give a very good qualitative picture of the phenomena. In the $\gamma \ll 1$ and $\gamma \gg 1$ limiting cases the general formula become the usual special formulae for the tunnel effect and multiphoton emission, respectively. In the transition region, where $\gamma \cong 1$, their accuracy is restricted, however, due to the simplified character of the models and to the approximations used; the calculated values of slope may not therefore be considered as exact. For example, according to [7, 8] a sufficient condition for the pure multiphoton case is $\gamma \gg 1$, while according to [25] a more stringent condition is needed: $\gamma \gg n_0$. Therefore in the investigated region of γ ($2.5 < \gamma < 12 = n_0$), the observation of the overwhelming tunnel-type character around, $\gamma \cong 4$ – remembering also the analogous case of atoms [12, 13] – is not a surprising fact.

In conclusion, we have observed laser-induced photoemission showing the features of the optical tunneling of electrons from gold surface, using single, mid-infrared ($\lambda \sim 2.94\,\mu\mathrm{m}$) high intensity ($5$–$120\,\mathrm{GW/cm^2}$) pulses of 110 ps. The light intensity dependence of the emitted electron current in the $1 < \gamma < 12$ range clearly differs from the previously demonstrated pure multiphoton and thermally assisted situations. The slope of the current dependences show typical optical tunneling features, and can be explained on the basis of the general Keldysh-theory of the photoemission. Further experimental efforts are necessary to study the $\gamma < 1$ case for metals, where interesting new properties of the emitted electrons (angular and energy distributions, coherence properties) can be expected.

Acknowledgements. The authors would like to thank Gy. Schmidt, J. Tóth and E. Sárközi for their technical help in the preparation of the target chamber, P. Bogár for his assistance during the experiments and also to acknowledge Prof. L.A. Kulevskii of the Institute of General Physics, Moscow, for providing the erbium laser system for the experiments. We thank Prof. A. Laubereau for his critical reading of the manuscript. This work was partly supported by the OTKA Foundation of the Hungarian Academy of Sciences, Grant #1783. One of the authors (K.L.V.) would like to thank the Alexander von Humbold Foundation for the partial support of his work.

References

1. Gy. Farkas: In *Photons and Continuum States of Atoms and Molecules*, ed. by N.K. Rahman, G. Guidotti, M. Allegrini (Springer, Berlin, Heidelberg 1987) p. 36
2. S.I. Anisimov, V.A. Benderskii, Gy. Farkas: Usp. Fiz. Nauk **122**, 185 (1977) [Sov. Phys. Usp. **20**, 467 (1977)]
3. Gy. Farkas, Z.Gy. Horváth: Opt. Commun. **12**, 392 (1974)
4. J.H. Bechtel, W.L. Smith, N. Bloembergen: Opt. Commun. **13**, 56 (1975)
5. R. Yen, J. Liu, N. Bloembergen: Opt. Commun. **35**, 277 (1980)
6. L.A. Lompré, J. Thébault, Gy. Farkas: Appl. Phys. Lett. **27**, 110 (1975)
7. L.V. Keldysh: Zh. Eksp. Teor. Fiz. **47**, 1945 (1964) [Sov. Phys. JETP **20**, 1307 (1965)]
8. F.V. Bunkin, M.V. Fedorov: Zh. Eksp. Teor. Fiz. **48**, 1341 (1965) [Sov. Phys. JETP **21**, 896 (1965)]
9. Gy. Farkas: In *Multiphoton Processes*, ed. by J.H. Eberly, P. Lambropoulos (Wiley, New York 1978) pp. 81–100
10. Gy. Farkas, S.L. Chin: Appl. Phys. B **37**, 141 (1985)
11. K.L. Vodopyanov, L.A. Kulevskii, Cs. Tóth, Gy. Farkas, Z.Gy. Horváth: Appl. Phys. B **48**, 485 (1989)
12. G. Gibson, T.S. Luk, C.K. Rhodes: Phys. Rev. A **41**, 5049 (1990)
13. M.D. Perry, O.L. Landen, A. Szöke, E.M. Campbell: Phys. Rev. A **37**, 747 (1988)
14. G.S. Arnold: Appl. Opt. **23**, 1434 (1984)
15. S.D. Pudkov: Zh. Tekh. Fiz. **47**, 649 (1977) [Sov. Phys. Tech. Phys. **22**, 389 (1977)]
16. L.D. Landau, E.M. Lifschits: *Electrodynamics of Continous Media* (Pergamon, Oxford 1984)
17. J.F. Ready: *Effects of High Power Laser Radiation* (Academic, New York 1971)
18. R.W. Shoenlein, W.Z. Lin, J.G. Fujimoto, G.L. Easley: Phys. Rev. Lett. **58**, 1680 (1987)
19. S.I. Anisimov, Yu.A. Imas, G.S. Romanov, Yu.V. Khodyko: *The Influence of High Power Radiation on Metals* (Nauka, Moscow 1970) (in Russian)
20. L.I. Andreeva, K.L. Vodopyanov, S.A. Kajdalov, Ju.M. Kalinin, M.E. Karasev, L.A. Kulevskii, A.V. Lukashev: Kvant. Elektron. **13**, 499 (1986) [Sov. J. Quantum Electron. **16**, 326 (1986)]
21. J.P. Girardeau-Montaut, C. Girardeau-Montaut: J. Appl. Phys. **65**, 2889 (1989)
22. Gy. Farkas, S.L. Chin, P. Galarneau, F. Yergeau: Opt. Commun. **48**, 275 (1983)
23. J.P. Girardeau-Montaut, C. Girardeau-Montaut: in Proc. Workshop on New Developments in Particle Acceleration Techniques, Orsay, France, 29 June–4 July, 1987, p. 516
24. S.T. Azizov, A.V. Zinovjev, V.B. Lugovskoi: Zh. Tekh.. Fiz. **51**, 1445 (1981) [Sov. Phys. Tech. Phys. **26**, 1509 (1981)]
25. A.P. Silin: Fiz. Tverd. Tela **12**, 3553 (1970) [Sov. Phys. Solid State **12**, 2886 (1971)]